# Human impact on river planform within the context of multi-timescale river channel dynamics in a Himalayan river system

Kim Vercruysse *, Robert C. Grabowski

*Cranfield Water Science Institute, School of Water, Energy and Environment, Cranfield University, MK43 0AL, United Kingdom*

A B S T R A C T

Rivers are dynamic landscape features which are often altered by human activity, making it difficult to disentangle human impact on geomorphic change from natural river dynamics. This study evaluated the human impact on river planform change within the context of short- and long-term river channel dynamics in the Himalayan Sutlej and Beas Rivers, by (i) systematically assessing river planform change over centennial, annual, seasonal and episodic timescales; (ii) connecting observed changes to human-environment drivers; and (iii) conceptualising these geomorphic changes in terms of timescale-dependent evolutionary trajectories (press, ramp, pulse). Landsat imagery was used to extract components of the post-monsoon active river channel (1989–2018), using the modified Normalized Differences Water Index to identify the wet river area, and visible red to determine active gravel bars. Findings were compared with a historical map to represent the pre-dam period (1847–1850) and with data on potential driving factors of change (discharge, climate and land cover). River planform characteristics changed significantly over all timescales, exhibiting strong spatiotemporal variation between and within both rivers. Dam construction likely caused channel narrowing and straightening at the centennial scale (press trajectory). In the Sutlej, this process has continued over the last 30 years, likely enforced by the cumulative effect of water abstraction and climatic changes (ramp trajectory). In the Beas, the pattern of change in river planform metrics was less pronounced over the same period and more variable along the length of the river, possibly linked to different dam operations that maintain a higher degree of flow variability and peak flows (press trajectory). High local erosion rates caused by aggregate mining (episodic) in the Sutlej were also observed (pulse trajectory). Expressed as evolutionary trajectories, the observed responses to human activity confirm the importance of legacy effects of human impact on river systems, and stress the dependency on spatial and temporal scales to determine trajectories of change. The multi-timescale assessment and conceptualisation provide insights into different dimensions of human impact on river planform change, which is pivotal to developing holistic management strategies.

## 1. Introduction

Alluvial rivers and their floodplains create and maintain a diversity of landscape features and habitats that provide a range of important ecosystem services (Felipe-Lucia et al., 2014; Gurnell et al., 2016; Van Looy et al., 2017; Wohl et al., 2019). Many of these river systems have been altered by humans, directly through the modification of channel and floodplains (e.g. re-sectioning and realignment) and indirectly through changes in water and sediment regimes (e.g. intensive agriculture, urbanisation, discharge regulation). These changes to river planform and geomorphic dynamics have caused, and continue to cause, ecological, hydrological and environmental impacts that propagate longitudinally (upstream/downstream) and laterally through the river system (Kuemmerlen et al., 2019). To minimize these negative impacts, it is important to quantify how river systems change in response to different processes and pressures. However, it is challenging to disentangle the relative and cumulative geomorphic impact of human activity within the context of multi-timescale river channel dynamics (Poeppl et al., 2017; Downs and Piégay, 2019).

Alluvial river systems are naturally dynamic landscape features as a result of interactions and feedback mechanisms between hydro-environmental processes. This complex system representing multi-scale controlling factors and processes can be conceptualised into the "three C's of rivers": connectivity, complexity, and context (Wohl et al., 2019). River connectivity is defined by the degree to which organisms and matter move longitudinally, laterally and vertically through the river corridor and wider catchment (Wohl, 2017). Connectivity is strongly driven by changes in the spatial heterogeneity (complexity) of the river system over multiple timescales (e.g. changes in land cover; Wohl, 2016). Finally, variations in connectivity and complexity form the basis for the spatial and temporal characteristics of river

* Corresponding author.
*E-mail address:* kim.vercruysse@joinforwater.ngo (K. Vercruysse).

reaches, eventually defining the geomorphic context of river corridors (e.g. river dimensions and shape, valley gradient and width, processes and fluxes of water, sediment, and other material) (Wohl, 2018).

Previous studies have investigated changes in the geomorphic context of rivers, and, in particular, how channel planform and geomorphic dynamics change over time in response to different factors (e.g. climate, human interventions). However, these geomorphic changes occur over different timescales, making it difficult to express them in terms of specific driving factors and processes (Llena et al., 2020). For example, long term (centennial to decadal) changes in river planform (i.e. dimensions and shape of river channel) have been studied extensively based on historical maps and remote sensing (Grabowski et al., 2014; Donovan et al., 2019; Langat et al., 2019; Joyce et al., 2020). These studies have shown that geomorphic behaviour and form of rivers across the world have changed strongly compared to a century ago due to land cover change and/or infrastructure construction (e.g. dams, embankments, irrigation canals), leading to e.g. lateral channel migration (Schwenk et al., 2017), channel narrowing (Cadol et al., 2011), channel straightening (Khan et al., 2018), and contributed to delta subsidence (Bravard et al., 2013; Manh et al., 2015). Similar types of change also occur over seasonal and/or episodic timescales, as a result of natural dynamics in a flashy river system with high sediment loads (Buendia et al., 2015; Rinaldi et al., 2016) or disturbance events (e.g. floods, bank erosion, landslides, storms, mining activity) (Croke et al., 2013; Janes et al., 2017; Llena et al., 2020).

Therefore, similar types of river change can be attributed to processes occurring over multiple timescales. The same magnitude of river channel change can occur naturally over decadal periods as over a couple of months. River channel narrowing and incision can occur over annual to decadal timescales due to the natural growth of vegetation, afforestation or dam construction (reduced erosion and sediment input) (Cadol et al., 2011; Coulthard and Van De Wiel, 2017), or over the course of a few months as a result of in-channel mineral mining, which may or may not recover after the activities have ceased (Rinaldi et al., 2005; Singh et al., 2016; Arróspide et al., 2018). To address this system of interacting processes and feedback mechanisms, previous studies have adopted multi-scale research designs to identify the impact of multiple disturbances (e.g. Schwenk et al., 2017; Llena et al., 2020). These studies have greatly improved understanding of cause-effect relations between human activities and geomorphic dynamics over multiple spatial and temporal scales (Downs and Piégay, 2019). Yet, because of the lack of data spanning multiple timescales, it remains difficult to assess the geomorphological importance of short-term (days to months) relative to long-term (years to decades) changes in river channel form and behaviour and how those changes relate to human impact. Due to data-availability issues and specific research designs, studies are often limited to a single timescale (e.g. decadal; Feeney et al., 2020), specific year(s) (e.g. areal imagery; Llena et al., 2020), or a pre-set time-interval (e.g. terrestrial laser scanner; Williams et al., 2014).

As observed changes in geomorphic dynamics in rivers are strongly timescale-dependent, limiting a geomorphic study to a single timescale can cause biased observations in channel dynamics, with long-term measurements leading to underestimations of the total change occurring over shorter timescales (Harvey and Gooseff, 2015; Donovan and Belmont, 2019). There is a need for consistent and explicit consideration of different timescales over which river systems change so that the spatiotemporal extent of human impacts can be characterised and evaluated. To this end, trajectories of change as defined in ecological sciences, expressed as *pulse* (temporary impact), *press* (permanent change of state), or *ramp* (continuous change) (Tello et al., 2010; Lake, 2013) (Fig. 1), present an excellent framework. Applying this classification to fluvial geomorphology should facilitate an improved understanding of rivers' variable and timescale-dependent evolutionary trajectories in response to multiple human activities (Wohl, 2018).

The resulting insights into the spatiotemporal variability in river change and associated human impact will help improve understanding
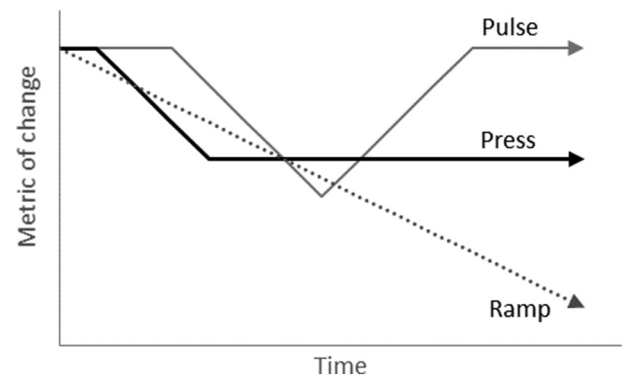


**Fig. 1.** Trajectories of change in response to ecological disturbances (modified from Tello et al., 2010). Applied to river planform change (e.g. narrowing of river planform), possible patterns of change are: (i) a rapid, permanent change (press), (ii) a gradual continuing change over time (ramp), and (iii) a short-term change after returning to the original state (pulse).

of possible future changes (Mould and Fryirs, 2018), and support the development of strategies to mitigate negative hydrological, ecological and socio-economic impacts associated with the degradation of riverine ecosystems (Poeppl et al., 2017). This understanding of river evolutionary trajectories is particularly important for Himalayan river systems, which are likely to be subject to further increased human impacts associated with economic growth and urbanisation (e.g. increasing demand for hydropower and resources such as water and aggregates), climate change (e.g. changes in flow amount and seasonality), and climate change adaptation (increased storage and diversions to meet irrigation and city demands) (Pandit and Grumbine, 2012; Momblanch et al., 2019).

This study aims to evaluate human impacts on river planform change within the context of short- and long-term river channel dynamics. To this end, the Himalayan Sutlej-Beas River system is used as a case study to (i) systematically assess changes in river planform characteristics over centennial, annual, seasonal, and episodic timescales; (ii) connect the observed patterns of planform change to human-environment drivers and interactions; and (iii) conceptualise these geomorphic changes in terms of timescale-dependant evolutionary trajectories (press, ramp, pulse).

## 2. Materials and methods

### 2.1. Study area

The study area was the Sutlej-Beas River system, which stretches from the Tibetan Autonomous Region in China, through the Indian states of Himachal Pradesh and Punjab, and joins the Indus River in Pakistan. The river system was selected because of its hydrological importance for the region. It is an active geomorphic system that has experienced major anthropogenic changes to water and sediment fluxes due to the construction of large hydro-electric dams and an extensive network of canals for water abstraction (Fig. 2). The study was conducted on the lower part of the catchment (11,992 km$^2$ in Sutlej and 2951 km$^2$ in Beas) below major dams on both rivers: Bhakra dam (construction: 1948–1963) and Pong dam (construction: 1961–1974) (Fig. 2). In these parts of the catchments, the rivers run through the wide plains of Punjab consisting of mainly Quaternary deposits (Geological Survey of India, 2007; Webb et al., 2011), which are primarily covered in rainfed and irrigated cropland with scattered patches of urban areas and grassland (Hollmann et al., 2013; Momblanch et al., 2019).

The Bhakra and Pong reservoirs are used to supply water for hydropower generation, irrigation, and regulation of high flows during the monsoon season (Momblanch et al., 2019) (Fig. 2). Despite heavy regulation, the hydrology of the rivers is still seasonally driven, with the
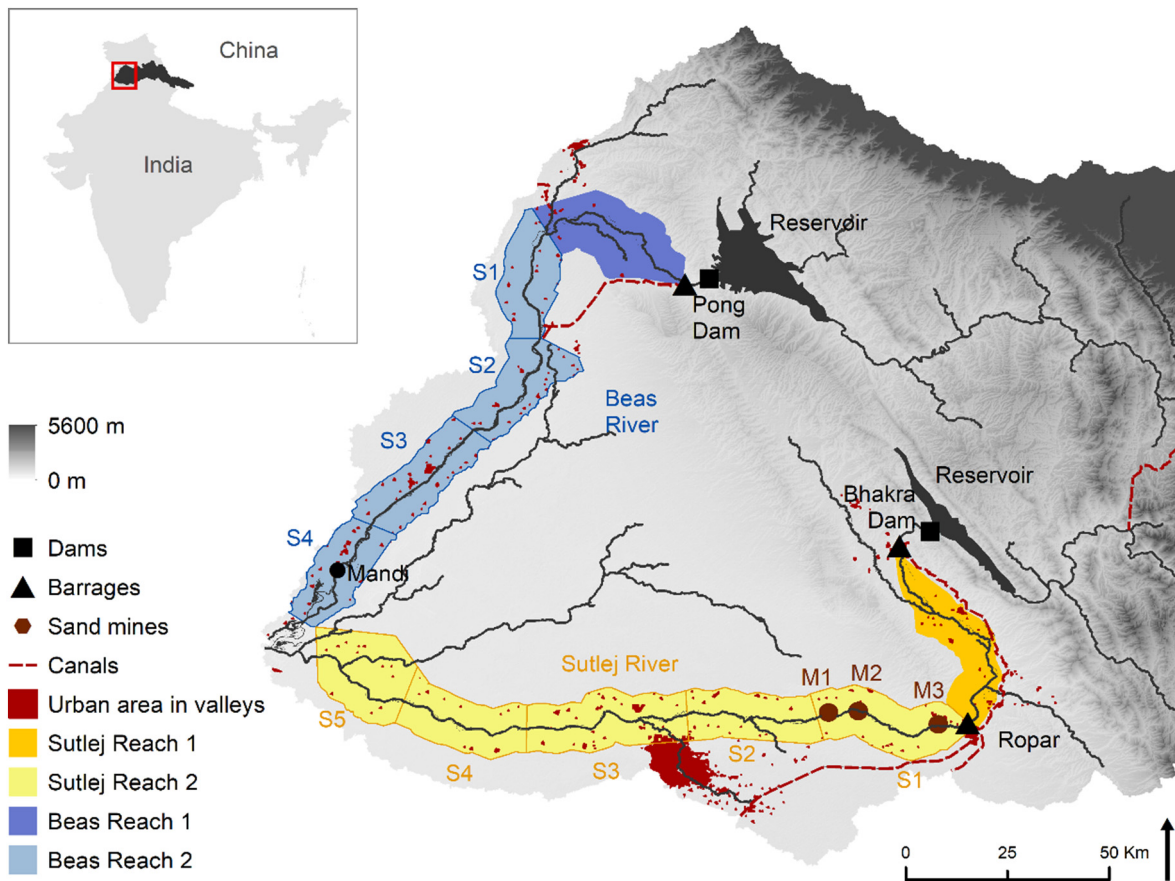
**Fig. 2.** Study area within the wider Sutlej and Beas catchment on the border between India and China, indicating the respective valleys and river reaches below barrages downstream of Pong and Bhakra dam. The lower reaches (Reach 2 of Sutlej and Beas) were each subdivided into sections (S1–4/5). Sand mining locations: Mandhala (M1), Lubangarh (M2) and Bramad Rail (M3). Mandi is the location of the monitoring station in the Global Monthly River Discharge Data Set (Vorosmarty et al., 1998).

lowest flows in winter (January–March), increasing flows in spring (April–May) due to snowmelt, which combines with monsoon rainfall in summer (June–September) to generate peak discharges. During the post-monsoon season (October–December), discharges gradually decrease again as rainfall reduces (Momblanch et al., 2019).

However, as a result of the large water control infrastructures on the river systems, the longitudinal connectivity of both rivers has been strongly altered. As commonly observed in rivers with large hydroelectric dams (Magilligan and Nislow, 2005; Richter et al., 2010), it is likely that river flow regimes in the Sutlej and Beas rivers have been altered due to the dams, including increased baseflow and decreased peak flow. While there are limited river gauging data available prior to the construction of the dams, the Global Monthly River Discharge Data Set (Vorosmarty

et al., 1998) provides a snapshot of river discharge prior to and post construction of the Pong Reservoir on the Beas River, near the confluence with the Sutlej. After the Pong dam construction was completed, monthly discharges became less variable between seasons and the minimum average monthly flow increased (from 120 to 300 m³/s) (Fig. 3).

Following these alterations to channel network connectivity and flow conditions, it is likely that the amount and frequency of sediment transported through the river system and geomorphic activity (channel bank and bed erosion and deposition) have also changed (Brandt, 2000). To investigate spatial differences in river planform, the rivers were classified into two reaches defined by their physiographic setting and valley gradient: (i) one reach downstream of the dams where the rivers flow through the mountain foothills (average gradient of
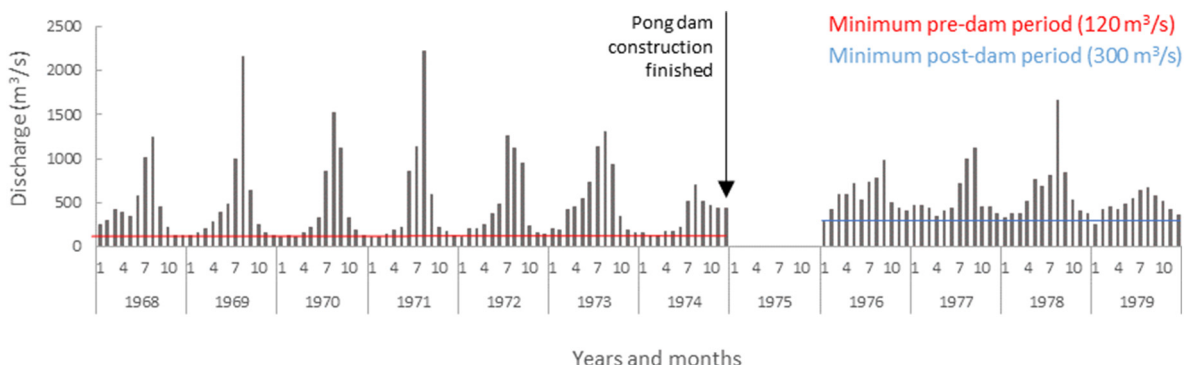


**Fig. 3.** Monthly average river discharge of Beas River at Mandi (Fig. 2) derived from the Global Monthly River Discharge Data Set (Vorosmarty et al., 1998).

0.0015) (Reach 1); and (ii) one reach representing the rivers flowing in the wider plains region (average gradient of 0.00035) (Reach 2) (Fig. 2). The reaches in the plains region (i.e. reach 2) were subdivided into smaller sections (~30 km) (sections 1–4/5).

### 2.2. River geomorphology

#### 2.2.1. Data

*2.2.1.1. Active channel mapping.* In this study, river planform dynamics were investigated by mapping two main components of the active river channel: the wet river area and active (un-vegetated) gravel bars during the post-monsoon season. In what follows, the method for mapping both components are described.

#### i. Wet river area

The wet river area was extracted automatically from satellite imagery of Landsat 5 to 8 (1989 to 2018) (Table 1). The extraction of wet area from satellite imagery is common practice, particularly when high resolution aerial imagery or topography data is missing (Langat et al., 2019; Boothroyd et al., 2021). The modified Normalized Difference Water Index (mDNWI) was used to differentiate water and land from the satellite imagery. It is a commonly used and well-tested method to extract river planforms and channel networks, which is calculated as: *(green band - mid infrared band)/(green band + mid infrared band))* (Isikdogan et al., 2017; Huang et al., 2018; Langat et al., 2019). Calculations of the mNDVI were performed using Google Earth Engine (GEE) based on imagery from the calibrated top-of-atmosphere (TOA) reflectance Landsat Image Collections within GEE (see data analysis section for dates of images) (Wang et al., 2018; Langat et al., 2019). The mNDWI raster images were reclassified to extract the wet river area, whereby mNDWI values higher than 0.15 were classified as water. Water pixels were given a value of one, while all other pixels were classified as no data (Fig. 4a-b). After additional editing to remove individual water pixels away from the river, the raster images were converted to polygon shapefiles (Fig. 4c) (Langat et al., 2019).

#### ii. Active gravel bars

Gravel bars are an important part of river channels that express the capacity of the river to perform geomorphic work and are an important component of high energy anabranching systems (Li et al., 2014; Rinaldi et al., 2016). However, no long-term data were available on the extent of gravel bars within the study area. To provide a preliminary indication of spatiotemporal dynamics in gravel bars, active (i.e. un-vegetated) gravel bars during the post-monsoon season were identified. To this end, visible red reflectance from the same Landsat 5 to 8 imagery was used to identify bare gravel bars (high reflectance) (Li et al., 2017; Forkuor et al., 2018). Only pixels within a buffer defined by the maximum extent of the wet river area over the observed period were considered (Fig. 4e). Based on visual inspection and comparison with high resolution imagery in Google Earth, raster pixels with values higher than 0.16 were reclassified as bare soil (Fig. 4d-e, Fig. I in supplementary material) and converted to shapefiles (Fig. 4f).

#### iii. Historic river planform

To allow comparison of the current river planform with the river planform before the Pong and Bhakra dams were built, a historic map of the region was used to characterize pre-dam river geomorphology. Multiple maps covering the region were identified in the British Library, but only one map (i) covered the entire study area, (ii) was created from surveys over a constrained and documented time period, and (ii) abided by standard British surveying conventions. The map is entitled "*The Trans-Sutluj Division, comprising the districts of Jalundhur, Hoshyarpoor and Kangra*" and was produced by the Revenue Survey of India between 1847 and 1852 (1 in.: 4 British Statute miles) (Revenue Survey of India, 1852). The map was geo-referenced with a topographical basemap in ArcGIS using nine hard-edged ground control points and a second order polynomial transformation (Grabowski and Gurnell, 2016; Donovan et al., 2019; Joyce et al., 2020). The riverbanks were manually digitized in GIS software to create a new polygon shapefile representing the river planform.

The geographical position of the channel in the historical map was not used for analysis because of (i) errors associated with the original drawing of the map which are impossible to quantify, (ii) uncertainties in geo-referencing to ground control points over a 150 year timespan, and (iii) the extended period of map creation (5 years), which means it cannot be used to link river forms to a location at a specific point in time. Therefore, metrics derived from the historic map should be considered as an indication of relative pre-dam river planform characteristics.

#### 2.2.1.2. River planform metrics

Based on the defined components of the active channel, metrics were calculated to characterize river planform change over time (Table 2). Each of the metrics was calculated for (i) both rivers in their entire length, (ii) the four reaches, and (iii) the nine sections.

**Table 1**
Data properties, title, resolution, extent used in this study, and references (Q: discharge).

| Subject | Properties | Title | Spatial resolution | Temporal resolution | Temporal extent | Reference |
|---|---|---|---|---|---|---|
| River geo-morhology | River planform | Revenue Survey of India | 1 in.: 4 mile | N/A | 1847–1850 | Revenue Survey of India, 1852 |
| | Active channel (wet river area and bars) | Landsat 4–5 TM TOA Refl. | 30 m | Weekly | 1989–1999 | (USGS/Google, 2020a) |
| | | Landsat 7 ETM+ TOA Refl. | 30 m | Weekly | 2000–2013 | (USGS/Google, 2020b) |
| | | Landsat 8 OLI TOA Refl. | 30 m | Weekly | 2013–2018 | (USGS/Google, 2020c) |
| | Sand mining | Sentinel-2 | 20 m | Weekly | 2016–2019 | (ESA, 2020) |
| Climate | Precipitation | TRMM (TMPA/3B43) Monthly rainfall rate | 0.25 arc deg. | Monthly | 1998–2019 | (Tropical Rainfall Measuring Mission (TRMM), 2011) |
| | Temperature | National Center for Environmental Prediction (NCEP) and National Center for Atmospheric Research (NCAR) | 0.25 arc deg. | Annual | 1990–2018 | (Kalnay et al., 1996) |
| Hydrology | Ropar Q | Daily discharge | N/A | Daily | 1999–2013 | Bhakra-Beas Management Board |
| | Bhakra Q | Daily discharge | N/A | Daily | 1989–2006 | Bhakra-Beas Management Board |
| | Pong Q | Daily discharge | N/A | Daily | 1989–2010 | Bhakra-Beas Management Board |
| Land cover | Vegetation | ESA Climate Change Initiative | 300 m | Annual | 1992–2015 | (Hollmann et al., 2013) |
| | Urbanisation | ESA Climate Change Initiative | 300 m | Annual | 1992–2015 | (Hollmann et al., 2013) |
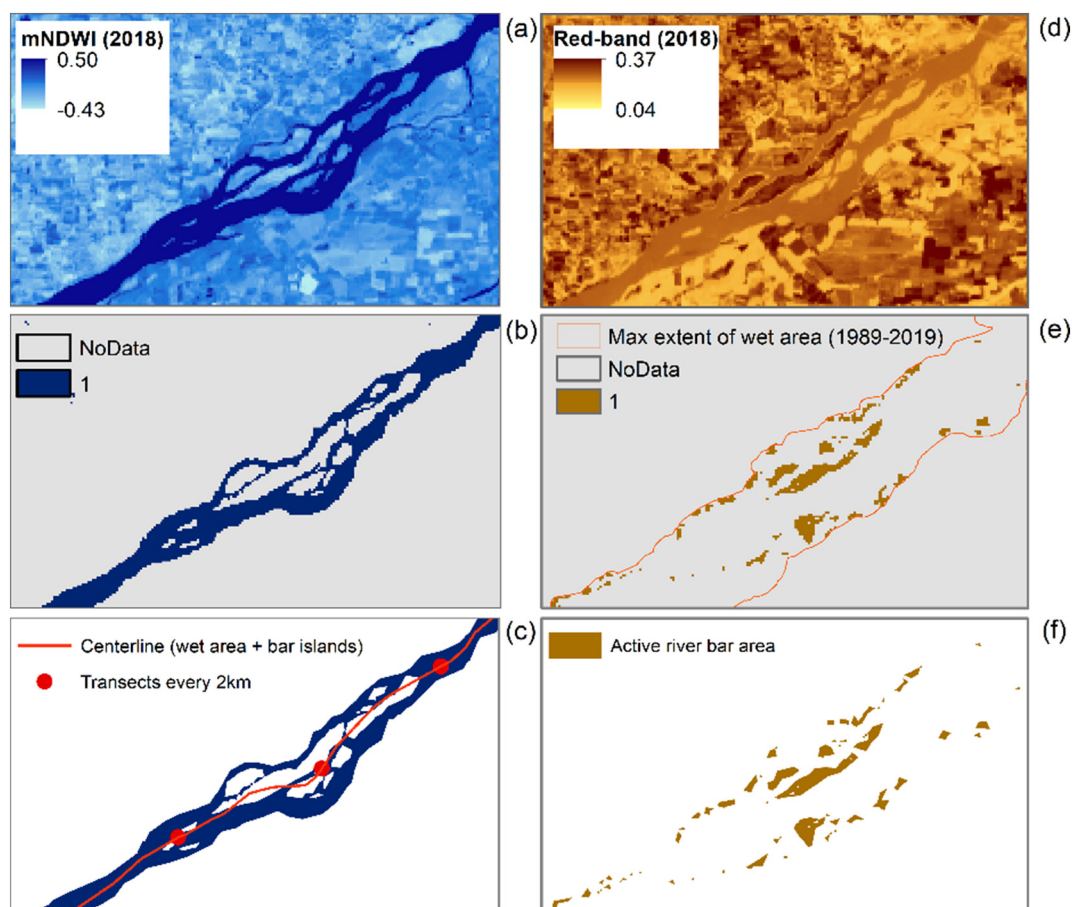
**Fig. 4.** Extraction of the wet river area and active gravel bars using remote sensing: (a) Landsat mNDWI imagery, (b) reclassification of mNDWI values (>0.15: water, rest: no data), (c) conversion from raster to wet river area polygon, (d) Landsat visible red imagery, (e) reclassification of reflectance values (>0.16: gravel bars, rest: no data) within a buffer defined by the maximal extent of all wet area polygons between 1989 and 2019, (f) conversion from raster to active gravel bar polygons.

First, the wet river area and active gravel bar area were calculated. Wet area was calculated as the total area (km$^2$) of the polygons extracted from the mNDWI images (Fig. 4c). Similarly, the active gravel bar area represents the total area (km$^2$) of the extracted polygons (Fig. 4f).

Active channel width was considered as the width of the wet area, including only gravel bars where they are entirely surrounded by water (i.e. islands) (Fig. 4c). This width was automatically calculated every 2 km with the Fluvial Corridor tool in ArcGIS (Roux et al., 2015) (Fig. 4c). While lateral bars would normally be included when measuring bankfull channel width (Demarchi et al., 2017), they were not included in the measurement of active channel width in this study, because the remotely sensed data does not permit the identification of all bars (both unvegetated and vegetated). Incorporation of only unvegetated bars in quantifying the channel width would therefore introduce errors.

The anabranching index was calculated to characterize the change in river form (Monegaglia et al., 2018).The index, which can

be applied to all multithread river systems (e.g. braiding and anastomosing), reflects the number of active channels separated by bars or islands, measured in at least 10 cross sections (spaced the width of one braid plain apart) (Marcinkowski et al., 2017; Monegaglia et al., 2018).

Finally, areas of erosion and deposition were quantified as the difference of the wet area polygons between two periods (see data analysis section for details on periods). Deposition was classified as the area of the wetted section that became dry land in the most recent period, while areas of erosion were identified as sections of the wet area that were classified as land in the previous period.

### 2.2.1.3. Aggregate mining activity

Aggregate mining in river channels is one example of a local, episodic, human activity that can have significant impacts on river geomorphology. Within the Sutlej-Beas catchment, aggregate mining is an increasing problem, with legal and illegal mining occurring, in

**Table 2**
River planform metrics.

| Metric | Definition | Unit |
|---|---|---|
| Wet river area | Total area of post-monsoon river polygon | km$^2$ |
| Active gravel bar area | Total area of post-monsoon gravel bar polygon | km$^2$ |
| Mean active channel width | Average width of active channel (wet river area + bar islands) based on transects every 2 km | m |
| Anabranching index | Number of active channels separated by bars or island, measured in at least 10 cross sections | No unit |
| Erosion | Area classified as land in the previous period based on the difference of river polygon area between two periods | km$^2$ |
| Deposition | Area that became dry land in the most recent period based on the difference of river polygon area between two periods | km$^2$ |

particular, in the lower part of the Sutlej River. An online government document with location names of 107 permitted mining locations from 2017 (Government of Punjab, 2017) was used as a guide to find locations with visible signs of mining activity on Google Earth for the available time-series of images (i.e. truck tracks and/or loaded trucks in the vicinity of distinct "carved-out" shapes along the river). From this visual analysis, 33 active mining locations were identified (Table I in supplementary material).

To assess the impact of mining activity on river geomorphology over time and compare its impact with long-term geomorphic change, ESA Sentinel-2 images were used (20 m resolution). The mNDWI was computed in GEE on imagery from the calibrated top-of-atmosphere (TOA) reflectance Sentinel-2 Image Collection (see data analysis section for dates of images). Initial comparison of the mNDWI imagery with Google Earth images containing known mining showed that only mining activity that impacts the border between water and land (i.e. carving away at the edge of sand bars) can be detected on the satellite (mNDWI) images (Fig. II in supplementary material). Three locations were selected to study in more detail that meet this criterion: Bramad Rail, Mandhala and Lubangarh (Fig. 2).

*2.2.2. Data analysis*

Changes in river planform were investigated over four timescales: centennial, annual, seasonal and episodic. For each timescale, data was analysed using a specific combination of imagery (Table 3). For the centennial and annual scale, images from the post-monsoon season were used to represent the annual river planform. The post-monsoon season has high water levels (i.e. at or near bankfull) and images have less cloud cover than the monsoon season, so a greater number of clear images can be used. For the analysis of seasonal variation in river planform, images were selected from five years where cloud-free images were available for each season (i.e. 1994, 2000, 2002, 2014 and 2018) (Table 3). Finally, for the episodic timescale, cloud-free images were selected from Sentinel-2. For all timescales, the available images within the selected time periods were averaged over months (or seasons) to ensure full spatial coverage of both rivers. In what follows, timescale specific data-analyses are further explained.

**i. Centennial**

The historic map (1847–1850) was used to calculate the metrics in Table 2 (except erosion and deposition) to characterize the general river planform dimensions during the pre-dam period. To represent the post-dam period, average values of the annual river planform metrics from 1989 to 2018 were calculated (based on annual post-monsoon river planforms derived from Landsat 5–8).

**ii. Annual**

The annual timescale provided the longest, most continuous dataset of river planform metrics (i.e. annual from 1989 to 2018), which allowed for a more in-depth time series analysis. Metrics (Table 2) were calculated for each year, which were then used to apply a Mann-Kendall trend analysis to detect significant monotonic trends in the annual time series (Martínez-Fernández et al., 2016). The statistical analysis was performed in the R environment (trend package). For reach 1 on the Sutlej River, the image of the post-monsoon season in 1997 contained gaps in the extracted polygons due to clouds so that the total planform area and metrics are likely underestimated for that year. The values for 1997 are shown in all figures illustrating the time-series, but were not included in the statistical trend analysis. In addition, no cloud-free imagery could be obtained for 1999 during the post-monsoon season.

**iii. Seasonal**

For selected years (Table 3), metrics were calculated for four seasons (winter, spring, monsoon and post-monsoon). Due to the discrete dataset, no trend analysis could be performed. The results of the seasonal analysis were interpreted in terms of how the magnitude of intra- and inter-seasonal variation and change in river metrics compared to the annual dynamics.

**iv. Episodic**

Aggregate mining activity along the river was used as an example of episodic change (i.e. not regularly occurring, change between months) in river planform. To this end, the erosion/deposition following mining activity was calculated based on average monthly wet river area for the three selected mining locations (Table 3). To avoid the influence of high monsoon flows on river planform changes, time periods were selected that exclude the monsoon season.

*2.3. Environmental dynamics*

*2.3.1. Data*

*2.3.1.1. Climate.* Climate can be a large-scale driving factor for geomorphic change (e.g. by increasing runoff or vegetation growth) (Dusar et al., 2011). Due to a lack of detailed time series of locally monitored climatic data within the study catchment, climatic data was collected based on remote sensing. GEE was used to compute average annual and seasonal temperatures (NCEP- NCAR) and rainfall rates (TRMM)

**Table 3**
Timescale, location, and period over which average Landsat/Sentinel-2 images were used to extract river planforms.

| Timescale | Location | Period | Imagery | Year(s) | mNDWI and visible red average |
|---|---|---|---|---|---|
| Centennial | Sutlej and Beas Rivers | Pre-dam | India Survey | 1847–1850 | N/A |
| | | Post-dam | Landsat 5–8 | 1989–2018 | Post-monsoon (Oct-Dec) |
| Annual | Sutlej and Beas Rivers | 29 years | Landsat 5–8 | 1989–2018 | Post-monsoon (Oct-Dec) |
| Seasonal | Sutlej and Beas Rivers | 5 years | Landsat 5–8 | 1994, 2000, 2002, 2014, 2018 | Winter (Dec – Mar) |
| | | | | | Spring (Mar – May) |
| | | | | | Monsoon (Jun – Sept) |
| | | | | | Post-monsoon (Oct-Dec) |
| Episodic | Sutlej River: Bramad Rail | 2 years | Sentinel-2 | 2016 | October |
| | | | | | November |
| | | | | 2017 | February |
| | Sutlej River: Mandhala | 2 years | Sentinel-2 | 2017 | October |
| | | | | | November |
| | | | | 2018 | February |
| | | | | | March |
| | Sutlej River: Lubangarh | 2 years | Sentinel-2 | 2017 | October |
| | | | | | December |
| | | | | 2018 | January |
| | | | | | March |

(Table 1). The values were spatially averaged for the Beas and Sutlej catchments.

*2.3.1.2. Hydrology.* Another factor controlling river geomorphology is linked to the hydrology of the river itself. Discharges into the rivers downstream of the Bhakra and Pong dams are heavily regulated. Monitoring data of these discharges were obtained from the Bhakra Beas Management Board (BBMB) for both dams, as well as for the barrage on the Sutlej River in Ropar (Fig. 2 and Table 1).

*2.3.1.3. Land cover.* Land cover data was collected as it can drive geomorphological river dynamics (Grabowski et al., 2014). Land cover data produced by ESA Climate Change Initiative (CCI) (2000 to 2015) was used (Table 1) (Hollmann et al., 2013). Because the focus of the study is on the impact of land cover on the rivers directly, only the land cover in the river valleys was used for analysis. River valleys were defined as the hillslopes most closely connected to the river channel, based on the method described by Cunha et al. (2018). Slopes within the catchment were first reclassified into three classes (hillslopes <10°, steep hillslopes 10–25°, and ridges >25°) and the cost-distance function in ArcGIS was then used to identify the hillslopes closest to the river channel until the point of inflection (natural break) where the slope changes towards steeper hillslopes. The valley polygons were then used to clip the selected satellite images. The classes from ESA CCI were reclassified into 4 classes: (i) annual vegetation (i.e. cropland) (including rain-fed and irrigated cropland, and mosaic cropland), (ii) permanent vegetation (including mosaic natural vegetation, tree cover, mosaic tree and shrub, mosaic herbaceous cover, shrub land, grassland), (iii) urban, and (iv) water.

### 2.3.2. Data analysis

Significant trends in the annual and seasonal time-series of temperatures, rainfall rates and discharge were determined using the Mann-Kendall trend analysis (Martínez-Fernández et al., 2016).

## 3. Results

### 3.1. River geomorphology

#### 3.1.1. Centennial

Comparison of river planform between the pre-dam (1847–1850) and post-dam period (1989–2018) reveal substantial change in characteristics (Fig. 5). Visual comparison suggests a general decrease in river planform dimensions and the development of canals to divert water from both rivers (Figs. 2 and 5). More specifically, the wet area and active channel width of both rivers have strongly decreased between the pre- and post-dam period (−63% and − 36% for Beas, −63% and − 50% for Sutlej, respectively) (Fig. 6).

The greatest difference between the pre- and post-dam river characteristics is the reduction in the number of side channels (i.e. anabranching index) of the Beas River immediately downstream of the Pong dam (−68% in reach 1 (foothills), compared to −20% in reach 2 (plains)) (Fig. 6a-d). The sections in reach 2 also show a variable pattern of change, whereby anabranching decreased in sections 1 and 3 but increased downstream in section 4. For the Sutlej River, the change was opposite, with less change in anabranching in foothills reach 1 (−28%), and a greater reduction in plains reach 2 (−46%) (Fig. 5 and 6d-f). All sections in the Sutlej reach 2 show a similar decrease.

#### 3.1.2. Annual

By refining the timescale of investigation to the annual scale, more detailed spatial patterns are observed. For the Beas River as a whole, there were no significant changes in wet area and active channel width during the observed period, except for the width of section 1 and area of section 1 to 3 (Fig. 7a-c, Table 4). The total area of active gravel bars along the Beas did decrease significantly, especially in reach 1. Contrarily, wet and gravel area and width of the Sutlej River decreased significantly for the entire river, both reaches, and almost all sections between 1989 and 2018 (Table 4, Fig. 7d-f).

Furthermore, similarly to the observed spatial variation between the two Beas reaches at the centennial scale, the decrease in anabranching was most pronounced in the foothill reach 1 (−71% compared to −48% in reach 2) (Fig. 7d, Table 4). Within reach 2, anabranching only significantly decreased in sections 3 and 4. The Sutlej River experienced a statistically significant decrease in anabranching in both reaches (reach 1: −17%, reach 2: −11%) (Table 4, Fig. 7g). In reach 2, anabranching decreased significantly only in section 2. Compared to the sections in the Beas reach 2, differences between sections were less pronounced in the Sutlej (Fig. 7e-f).

Finally, river planform dynamics were also expressed in annual deposition and erosion rates (Fig. 8). The magnitude of geomorphic activity was larger in the Sutlej than the Beas River, especially before the year 2000. While all reaches show a similar pattern of erosion and deposition, the magnitude of geomorphic activity was significantly higher in the lower plains reaches (reach 2), which is attributed to the larger size of these reaches compared to the upstream reaches. Note that the
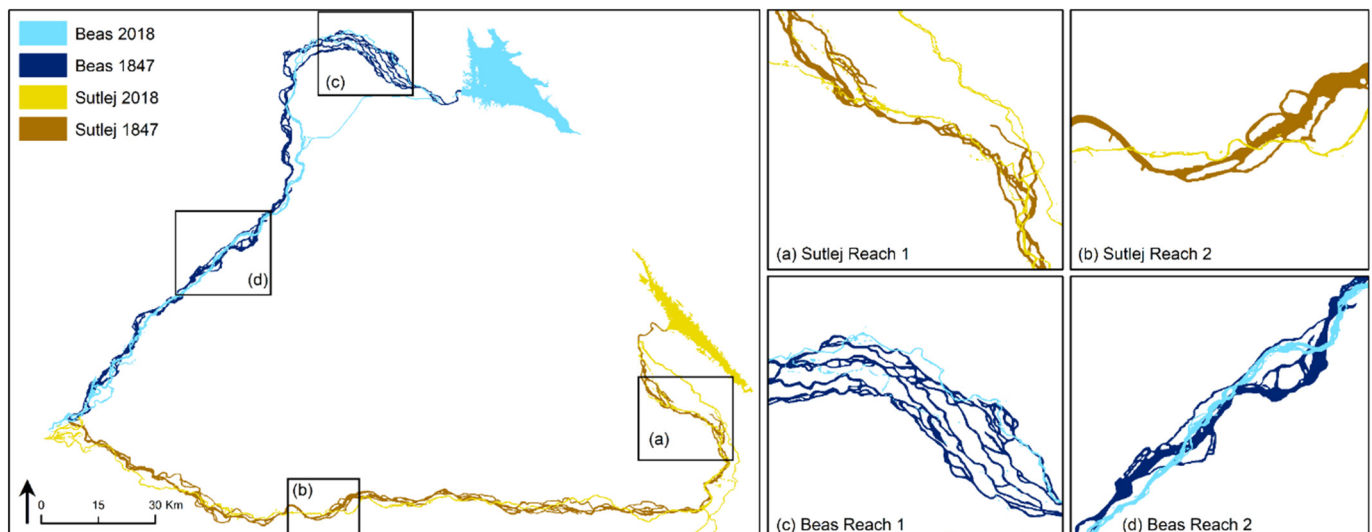


**Fig. 5.** Centennial river planform change for Beas and Sutlej Rivers: general overview of both rivers and close-up images of a river part in each of the four reaches.
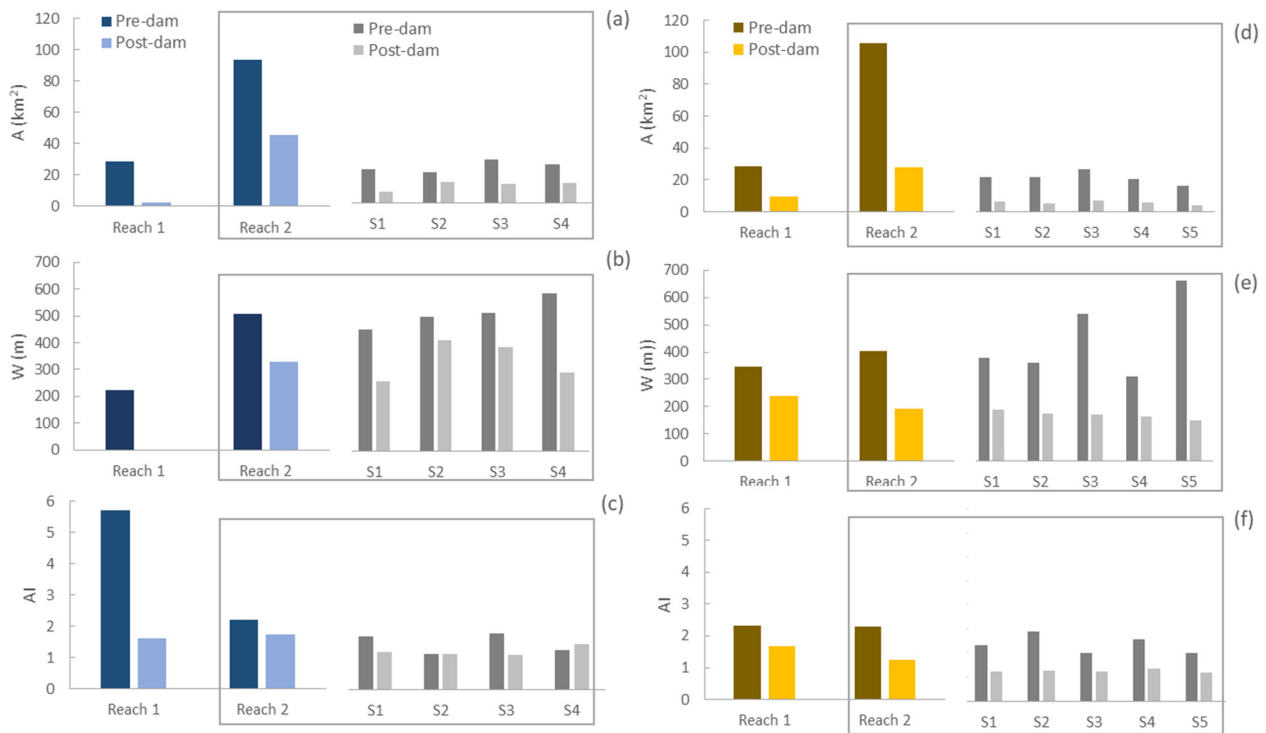
**Fig. 6.** Centennial change in wet river area (A), active channel width (W), and anabranching index (AI) for each river reach (1 and 2), and sections within reach 2 (S1-S4/5) for Beas (a-c) and Sutlej (d-f).

high deposition rates in 1996–1997 and erosion rates in 1997–1998 in the Sutlej are likely (partly) caused by the underestimation of river planform area in 1997 (due to incomplete cloud-free image cover).

*3.1.3. Seasonal*

No pronounced seasonal patterns were observed in the wet river area and active channel width of the Sutlej and Beas Rivers for the selected years (Fig. 9). Generally, the post-monsoon season is the time when the area and width is maximal, but large variation was not observed between seasons (except for 2018 in the Beas). In the Beas, the decrease in width and area across all selected years was most pronounced for the monsoon season, while in the Sutlej River, the winter area and width decreased most clearly.

*3.1.4. Episodic*

Substantial changes in planform where observed over short time-scales in the selected aggregate mining areas (Fig. 10). Changes followed a similar pattern at all three locations: channels were initially narrow (cream colour area, Fig. 10), but became increasingly wider over a period of five to six months. As the months progress, the river channel is gradually widened as river bars are being scraped away causing the newly created space to be filled with water (i.e. increasing area classified as water based on the mNDWI). Although other factors (e.g. natural bank erosion) cannot be excluded, visible mining activity on Google Earth during these time periods suggest most of the observed patterns are correlated to the removal of aggregates. The total area of eroded land (i.e. disappeared) was similar in Bramad Rail and Mandhala (0.09 km² in five months). In Lubangarh, the eroded land amounted 0.05 km² in six months.

*3.2. Environmental dynamics*

To help explain the observed change in river planform characteristics, environmental dynamics during the same period were investigated. Average annual temperatures were the same in both

catchments, so only one time series for the entire study area is shown (Fig. 11a). A slight increase in average annual temperature can be observed, which is confirmed by the Mann-Kendall test (Table 4). The monthly rainfall rate in both catchments does not show significant trends (Table 4). The average monsoon season rainfall rate shows pronounced peaks, indicating more rainy days and intense rainfall events (Figure11b). Finally, average daily dam discharges are generally higher in the Sutlej for all seasons compared to the Beas (Fig. 11c), while maximum daily discharges in the Beas are often higher than in the Sutlej (Fig. 11d). Only the post-monsoon discharge in the Beas shows a significant decreasing trend, while for the Sutlej winter discharge increased and monsoon season discharge decreased significantly (Table 4). Discharges at the Ropar barrage on the Sutlej follow a similar trend, but total discharges are lower than at the Bhakra dam on the Sutlej. For example, the average monsoon discharge during the monitored period at Ropar (155 m³/s) was 78% lower than at the Bhakra dam (737 m³/s) (Fig. 11c-e and Fig. 2).

Furthermore, land cover changes have occurred in both river valleys between 1992 and 2015 (Fig. 11 f-h, Table 4) Annual vegetation (cropland) along the Beas and Sutlej showed a slight, but statistically significant decreasing trend (−1.23% and -2.6%), while permanent vegetation very slightly increased by 0.43% and decreased by 0.14% for the Beas and Sutlej respectively. The most pronounced change in both valleys was the significant increasing trend in urbanisation (8.9% along the Beas and 2.7% along the Sutlej) (Table 4).

## 4. Discussion

This study investigated changes in river channel planform characteristics in a Himalayan river system over multiple timescales to assess human impact on river geomorphology. While similar changes were observed for both rivers, there were also differences in terms of temporal patterns of change between both rivers (e.g. annual trends, Fig. 7) or within the same river (i.e. foothills versus plains reaches), and in terms of spatial variation (e.g. different trends between reaches and
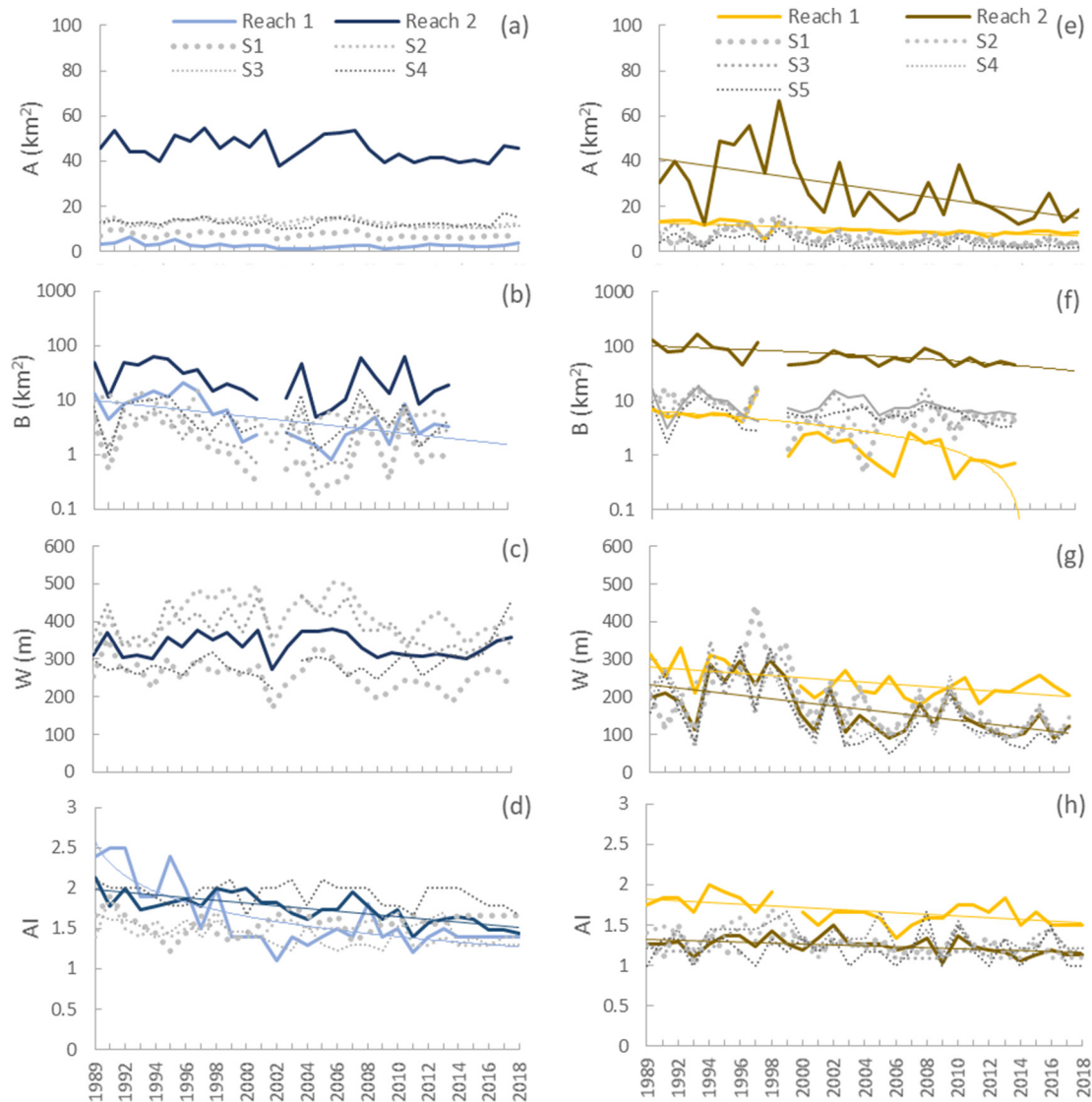
**Fig. 7.** Annual change in wet river area (A), active gravel bar area (B), active channel width (W), and anabranching index (AI) for each river reach (1 and 2), and sections within reach 2 (S1-S4/5) for Beas (a-c) and Sutlej (d-f). Solid trend lines indicate statistically significant decreasing trends (Mann-Kendall) in the reaches (Table 4).

sections in one river, Fig. 7). In what follows, the spatiotemporal variability is further discussed together with possible driving factors. Based on this discussion, evolutionary trajectories were conceptualised to illustrate the multiple dimensions of human impact on river geomorphology.

### 4.1. Spatiotemporal change and driving factors

#### 4.1.1. Centennial

At the centennial scale, observations mainly show the impact of dam construction on river geomorphology (Fryirs, 2013; Huang et al., 2013). The geomorphological impact of dams varies depending on the resulting discharge dynamics relative to sediment load, grain size, and river slope (Brandt, 2000; Geeraert et al., 2015). Specific to the Sutlej and Beas rivers, all considered metrics decreased between the pre- and post-dam period, indicating a reduction of side channels and channel narrowing (no data were available on incision) (Fig. 6). The longitudinal disconnectivity caused by the Bhakra and Pong dams and the reduction in magnitude of peak flows and sediment loads, have reduced the capacity of the river to perform geomorphic work (lateral migration of river) (Petts and Gurnell, 2005). Channel narrowing is a

common response to human disturbance in high-energy, braided rivers (Surian and Rinaldi, 2003), and similar types and magnitudes of changes have been observed (Gupta et al., 2012; Pal, 2016) or modelled (Sanyal, 2017) for other Himalayan and Asian river systems.

However, while the change in wet area and width was similar in both rivers, spatial differences were observed between the physiographic regions (i.e. foothills vs. plains reaches) and sections. The decrease in anabranching was most pronounced in the Beas reach directly downstream of the Pong dam (reach 1), while in the Sutlej, this change was most pronounced in the plains reach (reach 2). Because there are no notable geological differences between both reaches, this observation could be attributed to the tributary joining the Sutlej in reach 1, which dampened the effect of discharge and sediment reduction caused by the Bhakra dam (Fig. 2). A similar process could explain the spatial pattern in the Beas, as a tributary joins the river at the beginning on reach 2. In addition, land cover differences between the two catchments and reaches could also have played a role in causing variable responses to changes in flows (e.g. type of riparian vegetation) (Petts and Gurnell, 2005).

Moreover, while anabranching of all sections in the Sutlej reach 2 have decreased consistently with the decrease in the entire reach,

**Table 4**
Mann-Kendal (MK) trend analysis statistics for annual time-series (1989–2018) covering the entire river (River), reaches (1–2) and sections (S1–4/5) at the 95% confidence level. Trend (Tr): (−) decreasing, (+) increasing, (o) no trend, (/) no data. (A: wet river area, B: active gravel bar area, W: active channel width, AI: anabranching index, D: deposition, E: erosion, T: temperature, Q: discharge, L: land cover).

| Time series | | Beas | | Sutlej | |
|---|---|---|---|---|---|
| | | Tr | *p*-value | Tr | p-value |
| A | River | o | o | − | 0.00096 |
| | Reach 1 | o | o | − | 0.00002 |
| | Reach 2 | o | o | − | 0.00237 |
| | S1 | − | 0.04673 | − | 0.04673 |
| | S2 | − | 0.04274 | − | 0.00862 |
| | S3 | − | 0.01193 | − | 0.00616 |
| | S4 | o | o | − | 0.00616 |
| | S5 | / | / | − | 0.00342 |
| B | River | − | 0.04974 | − | 0.00187 |
| | Reach 1 | − | 0.006692 | − | 0.00004 |
| | Reach 2 | o | o | − | 0.00291 |
| | S1 | − | 0.00989 | − | 0.00870 |
| | S2 | − | 0.01272 | o | o |
| | S3 | o | o | − | 0.00187 |
| | S4 | o | o | o | o |
| | S5 | / | / | o | o |
| W | River | o | o | − | 0.00042 |
| | Reach 1 | / | / | − | 0.00236 |
| | Reach 2 | o | o | − | 0.00184 |
| | S1 | − | 0.04473 | − | 0.01193 |
| | S2 | o | o | − | 0.00109 |
| | S3 | o | o | − | 0.01326 |
| | S4 | o | o | − | 0.01633 |
| | S5 | / | / | − | 0.00580 |
| AI | River | o | o | o | o |
| | Reach 1 | − | 0.00072 | − | 0.00096 |
| | Reach 2 | − | 0.00001 | − | 0.00497 |
| | S1 | o | o | o | o |
| | S2 | o | o | − | 0.00002 |
| | S3 | − | 0.01437 | o | o |
| | S4 | − | 0.04617 | o | o |
| | S5 | / | / | o | o |
| D | River | o | o | − | 0.00973 |
| | Reach 1 | o | o | − | 0.01245 |
| | Reach 2 | o | o | o | o |
| | S1 | o | o | o | o |
| | S2 | o | o | o | o |
| | S3 | o | o | o | o |
| | S4 | o | o | o | o |
| | S5 | / | / | o | o |
| E | River | o | o | o | o |
| | Reach 1 | o | o | o | o |
| | Reach 2 | o | o | o | o |
| | S1 | o | o | o | o |
| | S2 | − | 0.03356 | o | o |
| | S3 | o | o | o | o |
| | S4 | o | o | o | o |
| | S5 | / | / | o | o |
| T | Average | + | 0.00002 | + | 0.00002 |
| | Winter | + | 0.00004 | + | 0.00004 |
| | Spring | + | 0.00410 | + | 0.00410 |
| | Monsoon | + | 0.00005 | + | 0.00005 |
| | Post-mons. | + | 9.7E-07 | + | 9.7E-07 |
| Q | Winter | o | o | + | 0.00573 |
| | Spring | o | o | o | o |
| | Monsoon | o | o | − | 0.00005 |
| | Post-mons. | − | 0.00256 | o | o |
| | Ropar winter | / | / | − | 0.00374 |
| | Maximum | − | 0.00002 | o | o |
| | Minimum | o | o | − | 0.00140 |
| L | Permanent veg. | + | 1.1E-11 | − | 6.7E-13 |
| | Annual veg. | − | 8.6E-10 | − | 3.0E-05 |
| | Urbanisation | + | 2.6E-08 | + | 6.7E-13 |

anabranching in section 4 in the Beas showed a slight increase in the post-dam period. These observations suggest a more complex and spatially-variable temporal response to human pressures on river planform dynamics in the Beas river. This type of response has also been

observed in other rivers (Marston et al., 2005) and becomes more apparent at the annual timescale.

### 4.1.2. Annual

The observed changes at the centennial scale suggest the geomorphic context of both rivers have changed with associated changes to river geomorphology. However, the data at the annual scale suggest that many river sections have not reached an equilibrium yet. The whole of the Sutlej River (entire river, reaches and sections) and the plains reach of the Beas River (reach 2) continued to lose wet river and active bar area, width, and anabranching over the last 30 years (Table 4 and Fig. 7).

These changes are likely the cumulative effect of several processes (Downs and Piégay, 2019). First, the continuing gradual decrease in river planform metrics is a common expression of legacy effects caused by dam construction (Wohl, 2015), whereby the decrease in sediment and flow variation caused continued river narrowing as the river tries to reach a new equilibrium. Similar findings have been observed for large rivers across the world, whereby quick change immediately after dam construction (within years) is followed by slow and continued change (over decades to centuries) (Brandt, 2000; Surian and Rinaldi, 2003), which has also been conceptualised in stream evolution models (Cluer and Thorne, 2014).

Second, apart from the impact of dam construction, other human activities may have had a compounding effect on the observed river planform changes. A significant declining trend in the average monsoon discharge was observed in the Sutlej (Table 4 and Fig. 11c). As there were no significant trends in precipitation, this decrease can be due to reduced dam releases and increased water abstraction through the canal systems (potentially enforced by increased evapotranspiration, i.e. rising temperatures, Fig. 11a). Especially in the plains reach (reach 2), abstraction at Ropar barrage can explain the 78% lower discharges entering the reach compared to the discharge entering reach 1 (Fig. 11c) (Asian Development Bank, 2011). No data were available on abstraction levels, but it is likely that economic growth and urbanisation in Punjab (Table 4 and Fig. 11h) and the neighbouring states relying on the Sutlej River for water provision have caused increased water demand and abstraction over the last 30 years (Ncube et al., 2018; Momblanch et al., 2019). The reduced flows would have led to decreased stream power (i.e. the energy of river to erode channel banks) (Wohl, 2018; Llena et al., 2020). The importance of high discharges for geomorphic activity in the Sutlej is illustrated by comparatively high erosion rates in 1994, 1995, and 1998 (Fig. 8), which correspond with three of the highest recorded daily peak discharges (1645, 1552, and 1329 m$^3$/s; Fig. 11). In addition, decreased variability in peak discharges in the Sutlej (Fig. 11d) could have led to decreased annual erosion and deposition rates (Fig. 8a-b). Furthermore, urbanisation also could have enforced the reduction in active gravel bars through increasing demand for land within the river valleys and gravel mining (Fig. 11).

Similar to the centennial scale, spatial differences in annual patterns of change were observed. Significant annual trends are generally absent for the Beas River as a whole (both reaches together), but there are substantial differences by physiographic region (reaches 1 and 2) and sections in the lower reach (reach 2) (Table 4). Reach 1 experienced a more sudden change in anabranching compared to reach 2 (and Sutlej reaches 1 and 2), while sections in reach 2 were characterised by variable trends and changes (Fig. 7). These spatial differences could be explained by a combination of factors. First, discharges released in the Sutlej were generally higher in all seasons than discharges released in the Beas River (Fig. 11c), which explains the overall higher geomorphic activity in the Sutlej (Fig. 8). However, peak discharges were higher in the Beas (Fig. 11d), which indicate that Pong dam is operated differently, maintaining a higher stream power at least intermittently or in response to natural factors and/or anthropogenic demands. These greater peak discharges could have caused the Beas to adjust quicker, explaining the lack of a clear continuing decrease. Second, no canal systems are (yet) in place to abstract water from the river further
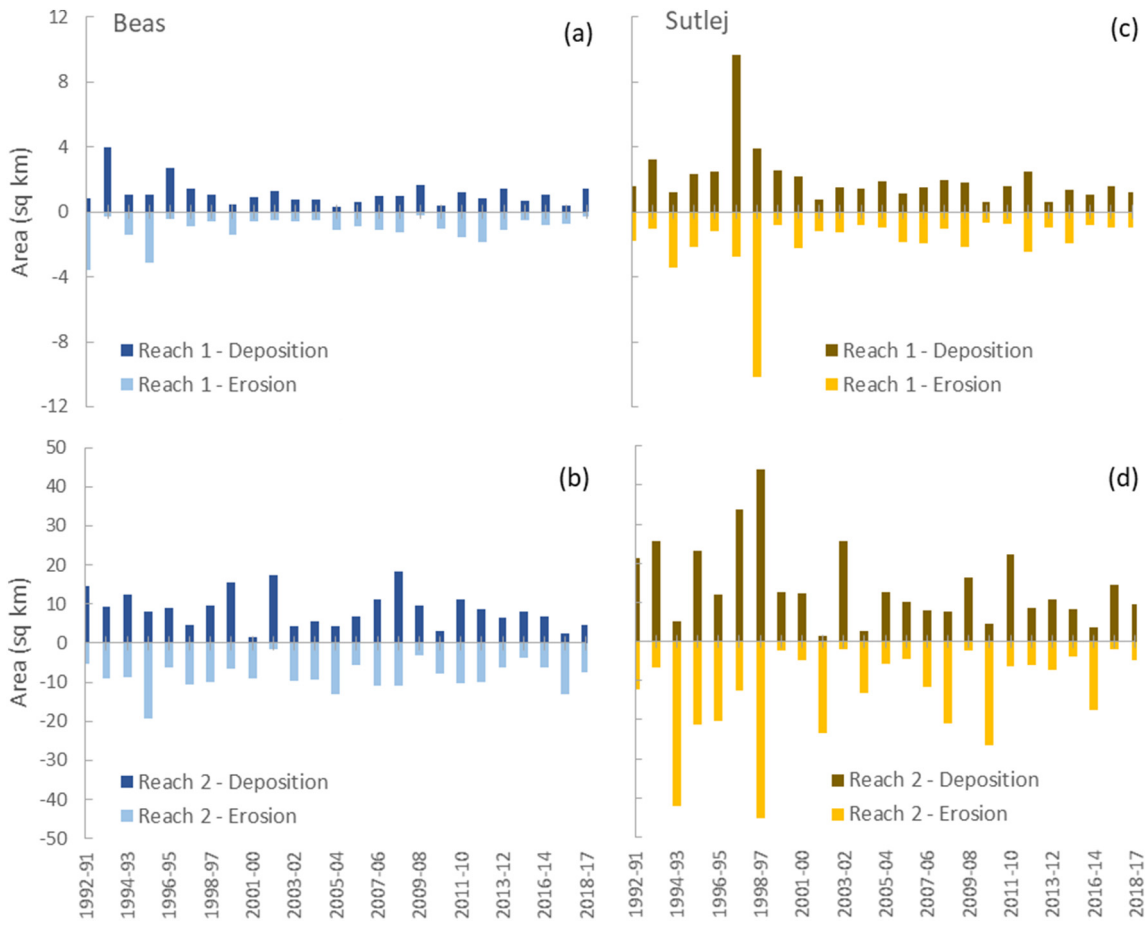
**Fig. 8.** Annual change in deposition and erosion of river planform of the Beas (a-b) and Sutlej (c-d) Rivers (difference between consecutive years) for reaches 1 and 2 respectively. Please note that because the lack of data in 1999, the annual values in 2000 represent the difference with 1998 (instead of 1999).

downstream of the Pong dam, eliminating the impact of water abstraction on channel narrowing as hypothesized for the Sutlej. Finally, the lower section (section 4) of the Beas flows towards Harike Wetland (Chopra et al., 2001). The wetland is a Ramsar site protected since 1990, which could explain the overall (and continuing) higher anabranching and active bar area in this section of the river (Fig. 7).
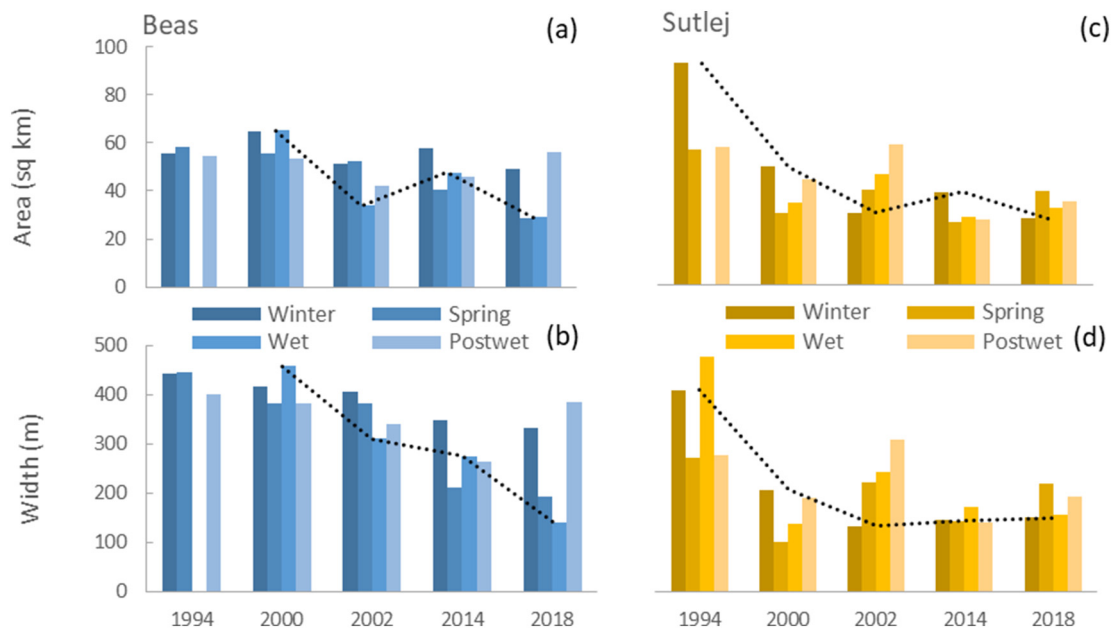


**Fig. 9.** Seasonal change in wet river area and mean active channel width in the Beas (a–b) and Sutlej (c–d) Rivers for selected years. Dotted black line emphasizes the decrease in monsoon area and width in the Beas River and in winter area and width in the Sutlej River.
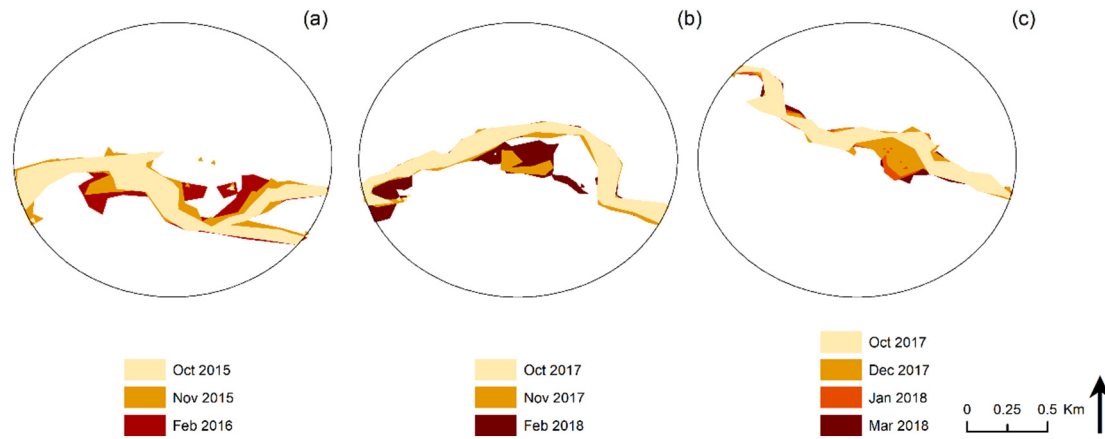
**Fig. 10.** Illustration of river planform erosion (widening) linked to sand/gravel mining activity for (a) Bramad Rail, (b) Mandhala, (c) Lubangarh.

#### 4.1.3. Seasonal

No clear seasonal patterns were observed for the selected years. The observed annual decline in wet area and active channel width is only expressed during the monsoon in the Beas and winter in the Sutlej (Fig. 8). These findings could be linked to an annual decreasing trend in maximum daily discharges (generally occur during monsoon) in the Beas and decreasing minimum daily discharges (generally occur during winter) in the Sutlej (Table 4 and Fig. 11).

Large differences between seasons were also not observed. There were no visible signs of consistently narrower active river channels during dryer periods (winter) (as might be expected in natural systems with a distinct monsoon period (Lawler et al., 1999)) (Fig. 8). These observations are typical characteristics of rivers with large dams and associated decreased seasonal variation in discharge (Fig. 2) (Magilligan and Nislow, 2005; Geeraert et al., 2018). However, the Beas exhibits again a different pattern, with more pronounced variation between seasons in wet area and width (Fig. 8a-b). These observations support the hypothesis that intra-annual discharges in the Beas remained more variable during the observed period.

#### 4.1.4. Episodic

Finally, while intra-annual variation in erosion was generally smaller than the annual variation, the results from the aggregate mining locations indicate that short-term variations can be significant (Fig. 9). Comparison of the three selected mines along the Sutlej indicate similar rates of erosion associated with aggregate mining. If the observed erosion quantities are considered representative for other mines, an average of 0.20 km$^2$ is being eroded annually in each mining location. Compared to an annual average of 20 km$^2$ for the entire Sutlej River (Fig. 8c-d), it would indicate that one mine can potentially cause around 1% of the total annual erosion (based on planform changes). Nevertheless, to date, the effect of aggregate mining is not reflected in the annual erosion rates (i.e. no significant increase in erosion in the Sutlej; Fig. 8), despite reports of increasing mining activity in rivers across India (Peduzzi, 2014; Pradesh and Choudhary, 2019).

#### 4.2. Timescale-dependent evolutionary trajectories

The construction of valley-spanning dams with large storage capacities on the neighbouring Sutlej and Beas Rivers would have been anticipated to have similar impacts on channel morphology over time. These large catchments are located in similar physiographic settings and climatic areas in the Himalayan foothills, and have experienced similar land cover changes. Therefore, the alteration of flow and sediment regimes would have been thought to cause similar timings and magnitudes of channel narrowing and loss of anabranching. However, this study quantified changes in river planform characteristics over long to short timescales that vary spatially across the river system. These changes can be expressed as temporal response patterns to human-environment processes that vary in type (gradual vs. abrupt), magnitude (centennial vs. seasonal) and space (Beas vs. Sutlej, foothills vs. plains), and can be conceptualised using the ecological terms ramp, press and pulse. We feel that application of these ecological terms facilitates the process-based description of the timescale-dependency of human impact on river geomorphology.

The observed patterns of change confirm the importance of legacy effects of human impact on river systems (Wohl, 2015) and indicate that a single driver (in similar rivers with similar human pressures) can result in different trajectories of change depending on the spatiotemporal scale and metric considered. When the analysis extends over the centennial timescale it suggests that a new geomorphic equilibrium has been reached, i.e. press response expressed as narrower, single-threat channels (Llena et al., 2020). However, the annual data indicate some degree of continuing change, i.e. ramp. In the Sutlej, reaches and most sections are characterised by a continued reduction in all considered metrics, suggesting the river is still adjusting to human influences. Conversely, significant annual decreasing trends were generally absent in the Beas, which suggests the river system has already adapted geomorphically to new boundary conditions imposed by human influences, exhibiting a press trajectory based on the available data and considered timescale. However, while changes along the Sutlej are relatively consistent in all sections, there is considerable spatial variation in the trajectories of change between sections in the Beas, suggesting a more complex interplay of controlling factors (e.g. proximity to protected areas, absence of abstraction points, local impact of urbanisation etc.).

Spatial variation in patterns of change stresses the need to also understand local pressures on geomorphology, such as aggregate mining. In the Sutlej there is no evidence, yet, that the extent and intensity of aggregate mining have crossed a threshold causing long-term responses in river geomorphology. Thus, at present, aggregate mining at its recent intensity can be described as a pulse trajectory at the episodic timescale. However, by only considering the very short timescale it is difficult to assess the actual geomorphic impact of this activity as part of long term change. Especially because aggregate mining in rivers have been shown to contribute to incision of the Mekong River and Delta (Vietnam) (Jordan et al., 2019) and the Po River (Italy) (Surian and Rinaldi, 2003) over decadal timescales.

#### 4.3. Suggestions for future research

Timescale-dependency in characterizing the rivers' evolutionary trajectories present considerable challenges in selecting scientific evidence most appropriate to manage and protect rivers and associated
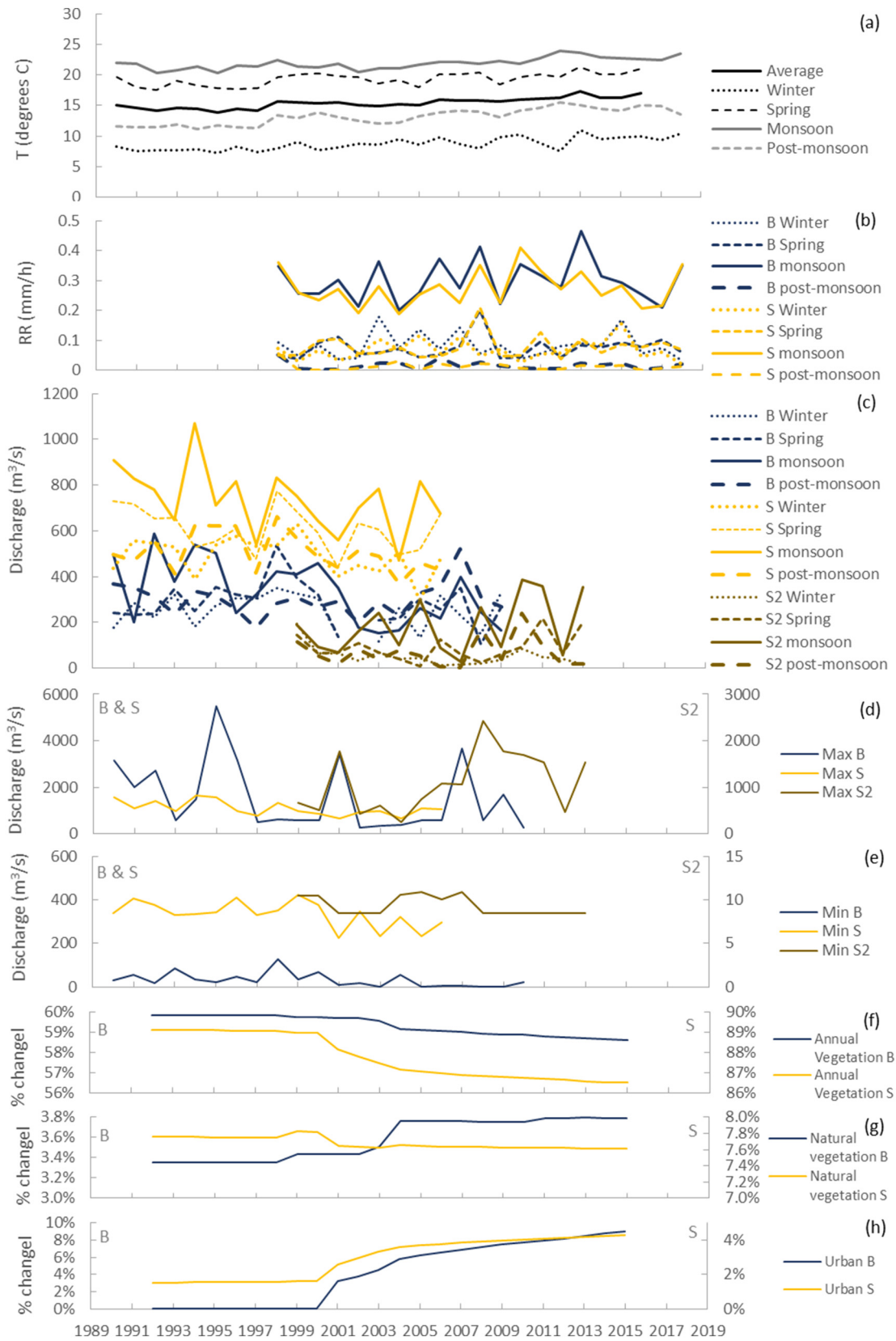
**Fig. 11.** Time series of (a) average annual and average seasonal temperatures for the entire study area; (b) average seasonal rainfall rates for Beas and Sutlej catchments; (c) seasonal average, (d) annual daily maximum, (e) annual daily minimum river discharge near outlet of Pong and Bhakra dam on Beas and Sutlej River (B is Beas, S is Sutlej and S2 is Ropar), and % land cover change: (f) annual vegetation, (g) permanent vegetation, (f) urban (the remaining percentage of the valleys consist of the water class).

ecosystems (Warmink et al., 2017). For example, by only considering long timescales (centuries to years), the potentially devastating impacts of short-term changes (e.g. habitat destruction due to aggregate mining (Koehnken et al., 2020)) are overlooked. Therefore, further research should focus on the geomorphic evolutionary trajectories of rivers over multiple timescales to support the development of holistic river management strategies (Mould and Fryirs, 2018).

Towards this end, we recommend future research to also focus on three main methodological aspects. First, this work could be repeated with more and higher resolution historical maps and/or remote sensing imagery (potentially focusing on smaller areas). In this study, data sources were selected to provide the best combination of spatial coverage and high temporal accuracy, but, as with most studies that investigate long-term geomorphic change over centuries or use automated extraction of remotely sensed data, there are uncertainties and limitations associated with the methodology (Grabowski and Gurnell, 2016; Joyce et al., 2020). Including more detailed imagery will allow to assess this uncertainty. In addition, more data will allow to better quantify the impact of aggregate mining.

Second, including more frequent remote sensing imagery is also recommended to investigate uncertainties associated with the methodology used to extract river planforms and gravel bars. Average post-monsoon imagery was used in this study. However, information extracted from satellite imagery can contain uncertainties resulting from the original imagery, classification, and timing of the image. As a result, geolocation errors and exceptionally wet or dry months might over- or underestimate derived metrics (Monegaglia et al., 2018).

Third, future research could build on this work by exploring other catchment dynamics in more detail (e.g. riparian vegetation dynamics, water abstraction rates), ideally through fieldwork (e.g. geomorphic mapping and vegetation analyses). These insights will help to address the current lack of detailed data on driving factors and to better understand the sequence of changes that occurred in different locations.

## 5. Conclusion

This study evaluated human impact on river planform change within the context of short- and long-term river channel dynamics in the Himalayan Sutlej-Beas River system. The results illustrate that river planforms characteristics significantly changed over centennial, annual, seasonal, and monthly timescales, exhibiting strong spatiotemporal variation between and within both rivers. These geomorphic dynamics can be conceptualised in terms of different evolutionary trajectories using the ecological terms ramp, press and pulse.

While the dominance of press-ramp trajectories confirms the importance of continuing legacy effects of human impact on river systems, the study also highlights that a single human impact can cause different trajectories depending on the spatiotemporal scale and metrics considered. The presented approach of conceptualising timescale-dependent evolutionary trajectories of geomorphic change in river systems can be applied to various geomorphic metrics in catchments with different geographic and human-environment interactions and pressures. The resulting insights will contribute to a better understanding of the multiple temporal dimensions of human impact on river planform change, which will inform development of holistic river management strategies.

## Declaration of competing interest

The authors declare that they have no known competing financial interests or personal relationships that could have appeared to influence the work reported in this paper.

## Data availability

No new data were collected in the course of this research and all spatial data can be accessed free of charge through Google Earth Engine.

## Appendix A. Supplementary data

Supplementary data to this article can be found online at https://doi.org/10.1016/j.geomorph.2021.107659.

## References

Arróspide, F., Mao, L., Escauriaza, C., 2018. Morphological evolution of the Maipo River in central Chile: influence of instream gravel mining. Geomorphology 306, 182–197. https://doi.org/10.1016/j.geomorph.2018.01.019.

Asian Development Bank, 2011. Appendix 2 lower Sutlej Sub Basin. TA 7417- IND: Support for the National Action Plan on Climate Change Support to the National Water Mission.

Boothroyd, R.J., Williams, R.D., Hoey, T.B., et al., 2021. Applications of Google Earth Engine in fluvial geomorphology for detecting river channel change. Wiley Interdiscip. Rev. Water 8, 1–27. https://doi.org/10.1002/wat2.1496.

Brandt, S.A., 2000. Classification of geomorphological effects downstream of dams. Catena 40, 375–401. https://doi.org/10.1016/S0341-8162(00)00093-X.

Bravard J-P, Goichot M, Gaillot S (2013) Geography of Sand and Gravel Mining in the Lower Mekong River. EchoGéo 0–20. doi:10.4000/echogeo.13659

Buendia C, Vericat D, Batalla RJ, Gibbins CN (2015) in-Channel Storage in a Highly Erodible Catchment. 1063:1045–1063.

Cadol, D., Rathburn, S.L., Cooper, D.J., 2011. Aerial photographic analysis of channel narrowing and vegetation expansion in Canyon De Chelly National Monument, Arizona, USA, 1935–2004. River Res. Appl. 27, 841–856. https://doi.org/10.1002/rra.1399.

Chopra, R., Verma, V.K., Sharma, P.K., 2001. Mapping, monitoring and conservation of Harike wetland ecosytem, Punjab, India, through remote sensing. Int. J. Remote Sens. 22, 89–98. https://doi.org/10.1080/014311601750038866.

Cluer, B., Thorne, C., 2014. A stream evolution model integrating habitat and ecosystem benefits. River Res. Appl. 30, 135–154. https://doi.org/10.1002/rra.2631.

Coulthard, T.J., Van De Wiel, M.J., 2017. Modelling long term basin scale sediment connectivity, driven by spatial land use changes. Geomorphology 277, 265–281. https://doi.org/10.1016/j.geomorph.2016.05.027.

Croke, J., Fryirs, K.A., Thompson, C., 2013. Channel-floodplain connectivity during an extreme flood event: implications for sediment erosion, deposition, and delivery. Earth Surf Process Landforms 38, 1444–1456. https://doi.org/10.1002/esp.3430.

Cunha, N.S., Magalhães, M.R., Domingos, T., et al., 2018. The land morphology concept and mapping method and its application to mainland Portugal. Geoderma 325, 72–89. https://doi.org/10.1016/j.geoderma.2018.03.018.

Demarchi, L., Bizzi, S., Piégay, H., 2017. Regional hydromorphological characterization with continuous and automated remote sensing analysis based on VHR imagery and low-resolution LiDAR data. Earth Surf Process Landforms 42, 531–551. https://doi.org/10.1002/esp.4092.

Donovan, M., Belmont, P., 2019. Timescale dependence in river channel migration measurements. Earth Surf Process Landforms 44, 1530–1541. https://doi.org/10.1002/esp.4590.

Donovan, M., Belmont, P., Notebaert, B., et al., 2019. Accounting for uncertainty in remotely-sensed measurements of river planform change. Earth-Science Rev 193, 220–236. https://doi.org/10.1016/j.earscirev.2019.04.009.

Downs, P.W., Piégay, H., 2019. Catchment-scale cumulative impact of human activities on river channels in the late Anthropocene: implications, limitations, prospect. Geomorphology 338, 88–104. https://doi.org/10.1016/j.geomorph.2019.03.021.

Dusar, B., Verstraeten, G., Notebaert, B., Bakker, J., 2011. Holocene environmental change and its impact on sediment dynamics in the eastern mediterranean. Earth-Science Rev 108, 137–157. https://doi.org/10.1016/j.earscirev.2011.06.006.

ESA (2020) Sentinel-2 MSI: MultiSpectral Instrument, Level-1C. https://earth.esa.int/web/sentinel/user-guides/sentinel-2-msi/product-types/level-1c

Feeney, C.J., Chiverrell, R.C., Smith, H.G., et al., 2020. Modelling the decadal dynamics of reach-scale river channel evolution and floodplain turnover in CAESAR-Lisflood. Earth Surf Process Landforms https://doi.org/10.1002/esp.4804.

Felipe-Lucia, M.R., Comín, F.A., Bennett, E.M., 2014. Interactions among ecosystem services across land uses in a floodplain agroecosystem. Ecol. Soc. 19. https://doi.org/10.5751/ES-06249-190120.

Forkuor, G., Dimobe, K., Serme, I., Tondoh, J.E., 2018. Landsat-8 vs. Sentinel-2: examining the added value of sentinel-2's red-edge bands to land-use and land-cover mapping in Burkina Faso. GIScience Remote Sens 55, 331–354. https://doi.org/10.1080/15481603.2017.1370169.

Fryirs, K.A., 2013. (Dis)Connectivity in catchment sediment cascades: a fresh look at the sediment delivery problem. Earth Surf Process Landforms 38, 30–46. https://doi.org/10.1002/esp.3242.

Geeraert, N., Omengo, F.O., Tamooh, F., et al., 2015. Sediment yield of the lower Tana River, Kenya, is insensitive to dam construction: Sediment mobilization processes in a semi-arid tropical river system. Earth Surf Process Landforms 40, 1827–1838. https://doi.org/10.1002/esp.3763.

Geeraert, N., Omengo, F.O., Tamooh, F., et al., 2018. Seasonal and inter-annual variations in carbon fluxes in a tropical river system (Tana River, Kenya). Aquat. Sci. 80, 0. https://doi.org/10.1007/s00027-018-0573-4.

Geological Survey of India (2007) Geological and mineral map of Punjab and Chandigarh.

Government of Punjab (2017) E-Auction notice.

Grabowski, R.C., Gurnell, A.M., 2016. Using historical data in fluvial geomorphology. In: Kondolf, G.M., Piegay, H. (Eds.), Tools in Fluvial Geomorphology. Wiley, pp. 56–74.

Grabowski, R.C., Surian, N., Gurnell, A.M., 2014. Characterizing geomorphological change to support sustainable river restoration and management. Wiley Interdiscip. Rev. Water 1, 483–512. https://doi.org/10.1002/wat2.1037.

Gupta, H., Kao, S.J., Dai, M., 2012. The role of mega dams in reducing sediment fluxes: a case study of large Asian rivers. J. Hydrol. 464–465, 447–458. https://doi.org/10.1016/j.jhydrol.2012.07.038.

Gurnell, A.M., Corenblit, D., Garcia de Jalon, D., et al., 2016. A conceptual model of vegetation-hydrogeomorphology interactions within river corridors. River Res. Appl. 32, 142–163. https://doi.org/10.1002/rra.2928.

Harvey, J., Gooseff, M., 2015. Consequences from bedforms to basins. Water Resour. Res. 51, 6893–6922. https://doi.org/10.1002/2015WR017617.

Hollmann, R., Merchant, C.J., Saunders, R., et al., 2013. The ESA climate change initiative: satellite data records for essential climate variables. Bull. Am. Meteorol. Soc. 94, 1541–1552. https://doi.org/10.1175/bams-d-11-00254.1.

Huang, F., Xia, Z., Li, F., Wu, T., 2013. Assessing sediment regime alteration of the upper Yangtze River. Environ. Earth Sci. 70, 2349–2357. https://doi.org/10.1007/s12665-013-2381-4.

Huang, C., Chen, Y., Zhang, S., Wu, J., 2018. Detecting, extracting, and monitoring surface water from space using optical sensors. A Review. Rev Geophys 56, 333–360. https://doi.org/10.1029/2018RG000598.

Isikdogan, F., Bovik, A., Passalacqua, P., 2017. RivaMap: an automated river analysis and mapping engine. Remote Sens. Environ. 202, 88–97. https://doi.org/10.1016/j.rse.2017.03.044.

Janes, V., Nicholas, A., Collins, A., Quine, T., 2017. Analysis of fundamental physical factors influencing channel bank erosion: results for contrasting catchments in England and Wales. Environ. Earth Sci. 76. https://doi.org/10.1007/s12665-017-6593-x.

Jordan C, Tiede J, Lojek O, et al (2019) Sand mining in the Mekong Delta revisited - current scales of local sediment deficits. Sci Rep 1–14. doi:10.1038/s41598-019-53804-z

Joyce, H.M., Warburton, J., Hardy, R.J., 2020. A catchment scale assessment of patterns and controls of historic 2D river planform adjustment. Geomorphology 354, 107046. https://doi.org/10.1016/j.geomorph.2020.107046.

Kalnay, E., Kanamitsu, M., Kistler, R., et al., 1996. The NCEP NCAR 40-Year Reanalysis Project. Bull. Am. Meteorol. Soc. 77, 437–472.

Khan, A., Rao, L.A.K., Yunus, A.P., Govil, H., 2018. Characterization of channel planform features and sinuosity indices in parts of Yamuna River flood plain using remote sensing and GIS techniques. Arab. J. Geosci. 11. https://doi.org/10.1007/s12517-018-3876-9.

Koehnken L, Rintoul MS, Acreman MC, et al (2020) Impacts of riverine sand mining on freshwater ecosystems: a review of the scientific evidence and guidance for future research. 1–9. doi:10.1002/rra.3586

Kuemmerlen, M., Reichert, P., Siber, R., Schuwirth, N., 2019. Ecological assessment of river networks: from reach to catchment scale. Sci. Total Environ. 650, 1613–1627. https://doi.org/10.1016/j.scitotenv.2018.09.019.

Lake, P.S., 2013. Resistance, resilience and restoration. Ecol. Manag. Restor. 14, 20–24. https://doi.org/10.1111/emr.12016.

Langat, P.K., Kumar, L., Koech, R., 2019. Monitoring river channel dynamics using remote sensing and GIS techniques. Geomorphology 325, 92–102. https://doi.org/10.1016/j.geomorph.2018.10.007.

Lawler, D.M., Grove, J.R., Couperthwaite, J.S., Leeks, G.J.L., 1999. Downstream change in river bank erosion rates in the Swale-Ouse system, northern England. Hydrol. Process. 13, 977–992. https://doi.org/10.1002/(SICI)1099-1085(199905)13:7<977::AID-HYP785>3.0.CO;2-5.

Li, Z., Wang, Z., Pan, B., et al., 2014. The development mechanism of gravel bars in rivers. Quat. Int. 336, 73–79. https://doi.org/10.1016/j.quaint.2013.12.039.

Li, H., Wang, C., Zhong, C., et al., 2017. Mapping urban bare land automatically from Landsat imagery with a simple index. Remote Sens. 9. https://doi.org/10.3390/rs9030249.

Llena, M., Vericat, D., Martínez-casasnovas, J.A., Smith, M.W., 2020. Geomorphic adjustments to multi-scale disturbances in a mountain river: a century of observations. Catena 192, 104584. https://doi.org/10.1016/j.catena.2020.104584.

Magilligan, F.J., Nislow, K.H., 2005. Changes in hydrologic regime by dams. Geomorphology 71, 61–78. https://doi.org/10.1016/j.geomorph.2004.08.017.

Manh N Van, Dung NV, Hung NN, et al (2015) Future sediment dynamics in the Mekong Delta floodplains: Impacts of hydropower development, climate change and sea level rise. Glob. Planet. Change 127:22–33. doi:https://doi.org/10.1016/J.GLOPLACHA.2015.01.001

Marcinkowski, P., Grabowski, R.C., Okruszko, T., 2017. Controls on anastomosis in lowland river systems: Towards process-based solutions to habitat conservation. Sci. Total Environ. 609, 1544–1555. https://doi.org/10.1016/j.scitotenv.2017.07.183.

Marston, R.A., Mills, J.D., Wrazien, D.R., et al., 2005. Effects of Jackson Lake Dam on the Snake River and its floodplain, Grand Teton National Park, Wyoming, USA. Geomorphology 71, 79–98. https://doi.org/10.1016/j.geomorph.2005.03.005.

Martínez-Fernández, V., Solana-Gutiérrez, J., González del Tánago, M., García de Jalón, D., 2016. Automatic procedures for river reach delineation: Univariate and multivariate approaches in a fluvial context. Geomorphology 253, 38–47. https://doi.org/10.1016/j.geomorph.2015.09.029.

Momblanch, A., Papadimitriou, L., Jain, S.K., et al., 2019. Untangling the water-food-energy-environment nexus for global change adaptation in a complex Himalayan water resource system. Sci. Total Environ. 655, 35–47. https://doi.org/10.1016/j.scitotenv.2018.11.045.

Monegaglia, F., Zolezzi, G., Güneralp, I., et al., 2018. Automated extraction of meandering river morphodynamics from multitemporal remotely sensed data. Environ. Model. Softw. 105, 171–186. https://doi.org/10.1016/j.envsoft.2018.03.028.

Mould, S., Fryirs, K., 2018. Contextualising the trajectory of geomorphic river recovery with environmental history to support river management. Appl. Geogr. 94, 130–146. https://doi.org/10.1016/j.apgeog.2018.03.008.

Ncube, S., Beevers, L., Adeloye, A.J., Visser, A., 2018. Assessment of freshwater ecosystem services in the Beas River Basin, Himalayas region, India. Proc Int Assoc Hydrol Sci 379, 67–72. https://doi.org/10.5194/piahs-379-67-2018.

Pal, S., 2016. Impact of Massanjore Dam on hydro-geomorphological modification of Mayurakshi River, Eastern India. Environ. Dev. Sustain. 18, 921–944. https://doi.org/10.1007/s10668-015-9679-1.

Pandit, M.K., Grumbine, R.E., 2012. Potential effects of ongoing and proposed hydropower development on terrestrial biological diversity in the Indian Himalaya. Conserv. Biol. 26, 1061–1071. https://doi.org/10.1111/j.1523-1739.2012.01918.x.

Peduzzi P (2014) Sand, rarer than one thinks. United Nations Environment Program (UNEP). 2012:1–15.

Petts, G.E., Gurnell, A.M., 2005. Dams and geomorphology: Research progress and future directions. Geomorphology 71, 27–47. https://doi.org/10.1016/j.geomorph.2004.02.015.

Poeppl, R.E., Keesstra, S.D., Maroulis, J., 2017. A conceptual connectivity framework for understanding geomorphic change in human-impacted fluvial systems. Geomorphology 277, 237–250. https://doi.org/10.1016/j.geomorph.2016.07.033.

Pradesh M, Choudhary V (2019) How will India address illegal sand mining without any data ? 1–13.

Revenue Survey of India (1852) The Trans-Sutluj Division, Comprising the Districts of Jalundhur, Hoshyarpoor and Kangra (catalogue number 52450 (33)). British Library.

Richter, B.D., Revenga, C., Scudder, T., et al., 2010. Lost in development's shadow: the downstream human consequences of dams. Water Altern 3.

Rinaldi, M., Wyzga, B., Surian, N., 2005. Sediment mining in alluvial channels: physical effects and management perspectives. River Res. Appl. 21, 805–828. https://doi.org/10.1002/rra.884.

Rinaldi, M., Gurnell, A.M., del Tánago, M.G., et al., 2016. Classification of river morphology and hydrology to support management and restoration. Aquat. Sci. 78, 17–33. https://doi.org/10.1007/s00027-015-0438-z.

Roux, C., Alber, A., Bertrand, M., et al., 2015. "FluvialCorridor": a new ArcGIS toolbox package for multiscale riverscape exploration. Geomorphology 242, 29–37. https://doi.org/10.1016/j.geomorph.2014.04.018.

Sanyal, J., 2017. Predicting possible effects of dams on downstream river bed changes of a Himalayan river with morphodynamic modelling. Quat. Int. 453, 48–62. https://doi.org/10.1016/j.quaint.2017.03.063.

Schwenk, J., Khandelwal, A., Fratkin, M., et al., 2017. High spatiotemporal resolution of river planform dynamics from landsat: the rivMAP toolbox and results from the Ucayali river. Earth Sp Sci 4, 46–75. https://doi.org/10.1002/2016EA000196.

Singh, R., Rishi, M.S., Sidhu, N., 2016. An overview of environmental impacts of riverbed mining in Himalayan Terrain of Himachal Pradesh. J. Appl. Geochem. 18, 473–479.

Surian, N., Rinaldi, M., 2003. Morphological response to river engineering and management in alluvial channels in Italy. Geomorphology 50, 307–326. https://doi.org/10.1016/s0169-555x(02)00219-2.

Tello, A., Corner, R.A., Telfer, T.C., 2010. How do land-based salmonid farms affect stream ecology? Environ. Pollut. 158, 1147–1158. https://doi.org/10.1016/j.envpol.2009.11.029.

Tropical Rainfall Measuring Mission (TRMM) (2011) TRMM (TMPA/3B43) Rainfall Estimate L3 1 month 0.25 degree x 0.25 degree V7. 10.5067/TRMM/TMPA/MONTH/7. Accessed 8 Jun 2020.

USGS/Google (2020a) USGS Landsat 5 TM Collection 1 Tier 1 TOA Reflectance. https://developers.google.com/earth-engine/datasets/catalog/LANDSAT_LT05_C01_T1_TOA#description. Accessed 8 Jun 2020.

USGS/Google (2020b) USGS Landsat 7 Collection 1 Tier 1 TOA Reflectance. https://developers.google.com/earth-engine/datasets/catalog/LANDSAT_LE07_C01_T1_TOA. Accessed 5 Jun 2020.

USGS/Google (2020c) USGS Landsat 8 Collection 1 Tier 1 TOA Reflectance. USGS Landsat 8 Collection 1 Tier 1 TOA Reflectance. Accessed 8 Jun 2020.

Van Looy, K., Tormos, T., Souchon, Y., Gilvear, D., 2017. Analyzing riparian zone ecosystem services bundles to instruct river management. Int J Biodivers Sci Ecosyst Serv Manag 13, 330–341. https://doi.org/10.1080/21513732.2017.1365773.

Vorosmarty CJ, Fekete BM, Tucker BA (1998) Global River Discharge, 1807-1991, V [ersion]. 1.1 (RivDIS).

Wang, C., Jia, M., Chen, N., Wang, W., 2018. Long-term surface water dynamics analysis based on landsat imagery and the Google Earth engine platform: a case study in the Middle Yangtze River Basin. Remote Sens. 10, 1635. https://doi.org/10.3390/rs10101635.

Warmink, J.J., Brugnach, M., Vinke-de Kruijf, J., et al., 2017. Coping with uncertainty in river management: challenges and ways forward. Water Resour. Manag. 31, 4587–4600. https://doi.org/10.1007/s11269-017-1767-6.

Webb, A.A.G., Yin, A., Harrison, T.M., et al., 2011. Cenozoic tectonic history of the Himachal Himalaya (northwestern India) and its constraints on the formation mechanism of the Himalayan orogen. Geosphere 7, 1013–1061. https://doi.org/10.1130/GES00627.1.

Williams, R.D., Brasington, J., Vericat, D., Hicks, D.M., 2014. Hyperscale terrain modelling of braided rivers: fusing mobile terrestrial laser scanning and optical bathymetric mapping. Earth Surf Process Landforms 39, 167–183. https://doi.org/10.1002/esp.3437.

Wohl, E., 2015. Legacy effects on sediments in river corridors. Earth-Science Rev 147, 30–53. https://doi.org/10.1016/j.earscirev.2015.05.001.

Wohl, E., 2016. Spatial heterogeneity as a component of river geomorphic complexity. Prog. Phys. Geogr. 40, 598–615. https://doi.org/10.1177/0309133316658615.

Wohl, E., 2017. Connectivity in rivers. Prog. Phys. Geogr. 41, 345–362. https://doi.org/10.1177/0309133317714972.

Wohl, E., 2018. Geomorphic context in rivers. Prog. Phys. Geogr. 42, 841–857. https://doi.org/10.1177/0309133318776488.

Wohl, E., Brierley, G., Cadol, D., et al., 2019. Connectivity as an emergent property of geomorphic systems. Earth Surf Process Landforms 44, 4–26. https://doi.org/10.1002/esp.4434.